American Journal of Botany 96(5): 865–876. 2009.

IN VIVO STUDY OF DEVELOPMENTAL PROGRAMMED CELL DEATH USING THE LACE PLANT (*APONOGETON MADAGASCARIENSIS*; APONOGETONACEAE) LEAF MODEL SYSTEM[1]

HARRISON WRIGHT,[2,3] WOUTER G. VAN DOORN,[4] AND ARUNIKA H. L. A. N. GUNAWARDENA[3,5]

[2]Atlantic Food and Horticulture Research Center, Agriculture and Agri-Food Canada, Kentville, Nova Scotia, B4N 1J5, Canada;
[3]Department of Biology, Dalhousie University, Halifax, Nova Scotia, B3H 4J1, Canada; and
[4]Mann Laboratory, Department of Plant Sciences, University of California, Davis, California, 95616 USA

Programmed cell death (PCD) is required for many morphological changes, but in plants it has been studied in much less detail than in animals. The unique structure and physiology of the lace plant (*Aponogeton madagascariensis*) is well suited for the in vivo study of developmental PCD. Live streaming video and quantitative analysis, coupled with transmission electron microscopy, were used to better understand the PCD sequence, with an emphasis on the chloroplasts. Dividing, dumbbell-shaped chloroplasts persisted until the late stages of PCD. However, the average size and number of chloroplasts, and the starch granules associated with them, declined steadily in a manner reminiscent of leaf senescence, but distinct from PCD described in the *Zinnia* tracheary element system. Remaining chloroplasts often formed a ring around the nucleus. Transvacuolar strands, which appeared to be associated with chloroplast transport, first increased and then decreased. Mitochondrial streaming ceased abruptly during the late stages of PCD, apparently due to tonoplast rupture. This rupture occurred shortly before the rapid degradation of the nucleus and plasma membrane collapse, in a manner also reminiscent of the *Zinnia* model. The presence of numerous objects in the vacuoles suggests increased macro-autophagy before cell death. These objects were rarely observed in cells not undergoing PCD.

Key words: *Aponogeton madagascariensis*; Aponogetonaceae; autophagy; chloroplast; cytoplasmic streaming; lace plant; light microscopy; programmed cell death; transmission electron microscopy; transvacuolar strands.

Programmed cell death (PCD) is an integral part of plant development and defense. Essential for the normal functioning of plants, PCD may be found throughout the life cycle, from the fertilization of the ovule, to the formation of the xylem, to the death of the whole plant (van Doorn and Woltering, 2005).

The aquatic lace plant [*Aponogeton madagascariensis* (Mirbel) H. Bruggen] (Fig. 1A) is an excellent model system for the study of developmental PCD in plants (Gunawardena et al., 2004, 2006, 2007; Gunawardena, 2008). Leaf venation in this species is somewhat peculiar because it consists of a network of longitudinal and transverse veins, enclosing segments (called areoles) that are roughly square. Perforations form in the middle of these areoles as a result of the death of specific cells. PCD is induced first in the center cells of the areoles and later in cells that are closer to the veins, while the cells within five cell layers of the veins do not die (Gunawardena et al., 2004). The tissue of the areoles is only four cell layers thick: two epidermal layers enclose two mesophyll cell layers.

The developmental morphology of the lace plant leaf can be broken down into five stages: (1) pre-perforation, (2) window formation (Fig. 1B), (3) perforation formation, (4) perforation expansion, and (5) mature perforation. It is during the window formation stage that a discrete population of cells predictably undergoes PCD (Gunawardena et al., 2004). The genetically regulated, systematic degradation of cells that occurs during development in this species carries many of the hallmarks of PCD: invagination and shrinkage of the plasma membrane (PM) and nuclear membrane, condensation of the cytoplasm, TUNEL positive nuclei indicating DNA fragmentation (Gunawardena et al., 2004), presence of reactive oxygen species (ROS) (Gunawardena et al., 2007), presence of caspase-like activity, and the inhibition of PCD by ethylene inhibitors (A. Gunawardena, unpublished data).

Although much work has been done to associate plant PCD with changes to the vacuole, nucleus, and mitochondria (Groover et al., 1997; Kuriyama, 1999; Balk and Leaver, 2001; Obara et al., 2001), little is known about the changes and potential role of the chloroplasts. Thus far, the fate of chloroplasts has been studied mainly during the developmental PCD of leaves that yellow at the end of the growing season (i.e., leaf senescence; Inada et al., 1998, 1999). The PCD that occurs in the lace plant system is reminiscent of the differentiation of isolated *Zinnia* leaf mesophyll cells into tracheary elements (TEs) (Fukuda et al., 1998). It is now widely accepted that the moment the cell dies during PCD is the time of vacuolar collapse, i.e., permeabilization or rupture of the tonoplast (Jones et al., 2001; van Doorn and Woltering, 2004). In the *Zinnia* model, it was inferred that organelles were degraded only after the rupture of the tonoplast, which releases hydrolases from the vacuole. First, the ER and Golgi bodies disappear, followed by the chloroplasts and mitochondria. The chloroplast matrix is

[1] Manuscript received 9 October 2008; revision accepted 5 January 2009.

The authors thank N. Dengler for reviewing this article, G. Rantong for artwork, and V. Hannon for assistance in formatting supplementary videos. The authors thank the Natural Sciences and Engineering Research Council (NSERC) of Canada for Canadian Graduate Studies doctoral funding (CGS D) for H.W. and a discovery and equipment grant for A.G.

[5] Author for correspondence (e-mail: arunika.gunawardena@dal.ca)

doi:10.3732/ajb.0800343

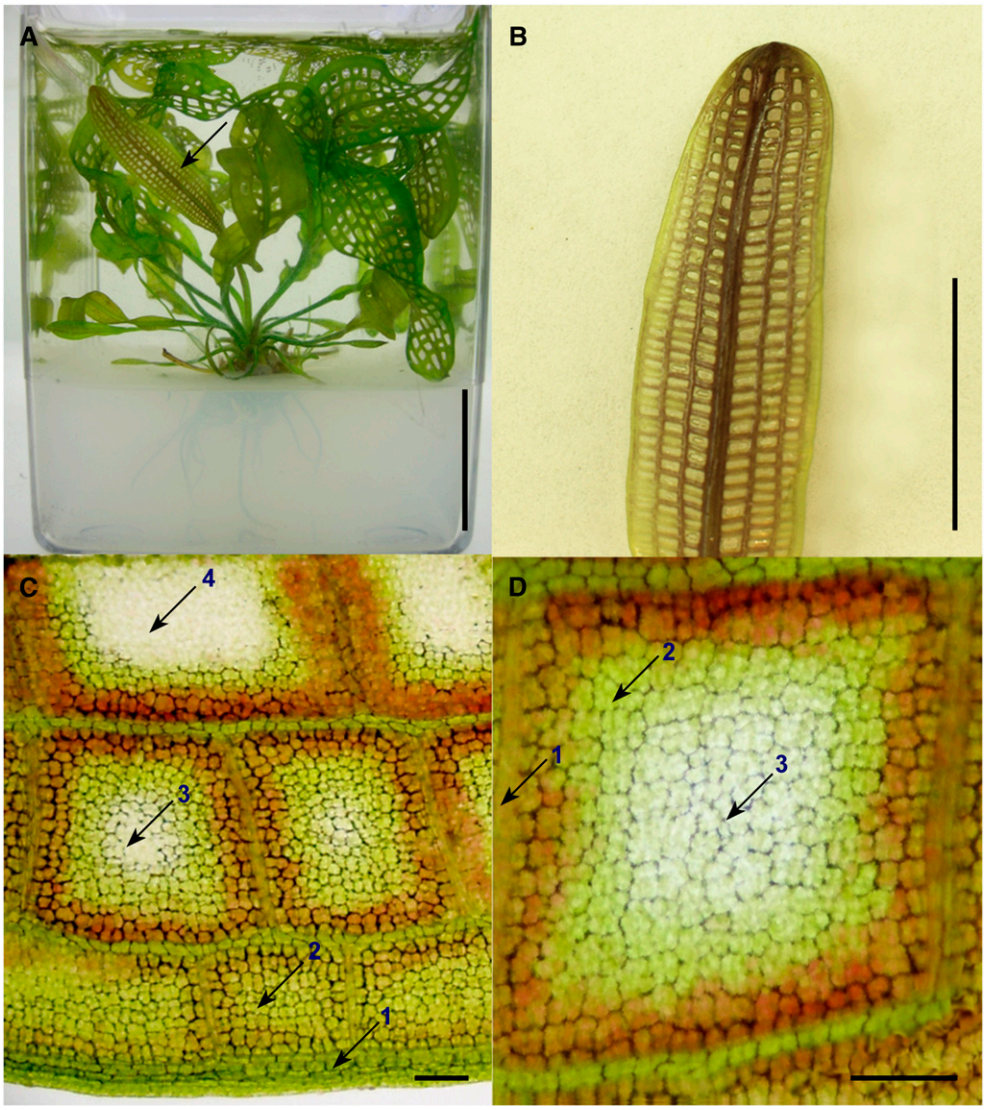

Fig. 1. Light micrographs of the morphology of developing lace plant leaf. (A) Lace plant with window formation leaf (arrow) growing in axenic culture in a magenta box. (B) Window formation/early perforation formation lace plant leaf. (C) Stages 1a–4a of programmed cell death (PCD) within a single leaf. (D) Stages 1b–3b of PCD within a single window. Bars = 2 cm in (A), 1 cm in (B) and 200 μm in (C) and (D).

degraded first, then the internal membrane structure (Fukuda et al., 1998).

During leaf senescence, the chloroplasts are slowly degraded from within. They lose chlorophyll, stroma, and stroma thylakoids (Ljubesic, 1968; Sakamoto, 2006; Hörtensteiner and Lee, 2007). A chloroplast that has lost its chlorophyll and most of its internal structure is called a gerontoplast. During leaf senescence, the gerontoplasts form long before rupture of the tonoplast. In contrast to the *Zinnia* TE PCD system, most chloroplasts disappear before the cells die.

The purpose of the current study was to showcase the use of in vivo, live streaming video microscopy and a quantitative approach in determining the developmental PCD execution process of the novel lace plant system. Emphasis was placed on determining the relative timing of apparent autophagic activity, chloroplast destruction, and tonoplast collapse and on comparing this system to others.

MATERIALS AND METHODS

Plant material—Lace plants for quantitative analyses were grown in axenic culture in magenta boxes (Fig. 1A) as described by Gunawardena et al. (2006). Plants were maintained at 25°C with 12 h light/12 h dark cycles provided by daylight fluorescent bulbs (Philips, Daylight Deluxe, F40T12/DX, Markham, Ontario) at ≈125 $\mu mol \cdot m^{-2} \cdot s^{-1}$. Leaf samples in the mid window formation stage of leaf development (Fig. 1B), as defined by Gunawardena et al. (2004), were selected for measurement. For comparison, additional general observations were also made on window formation stage leaves stained for 1 h with Evans blue (0.5% w/v water), unstained, window formation stage, aquarium-grown lace plant leaves (125 L tank, 12 h light/12 h dark cycles provided by daylight fluorescent bulbs [Eclipse, natural daylight, F30T8, Nuremberg, Germany] at ≈125 $\mu mol \cdot m^{-2} \cdot s^{-1}$ [including actinic light from a window]) and unstained mature perforation stage leaves from plants grown in magenta boxes.

PCD stages delineated within a leaf, window, and over time—Lace plant leaves grown in a magenta box (Fig. 1A) often develop four parallel longitudinal

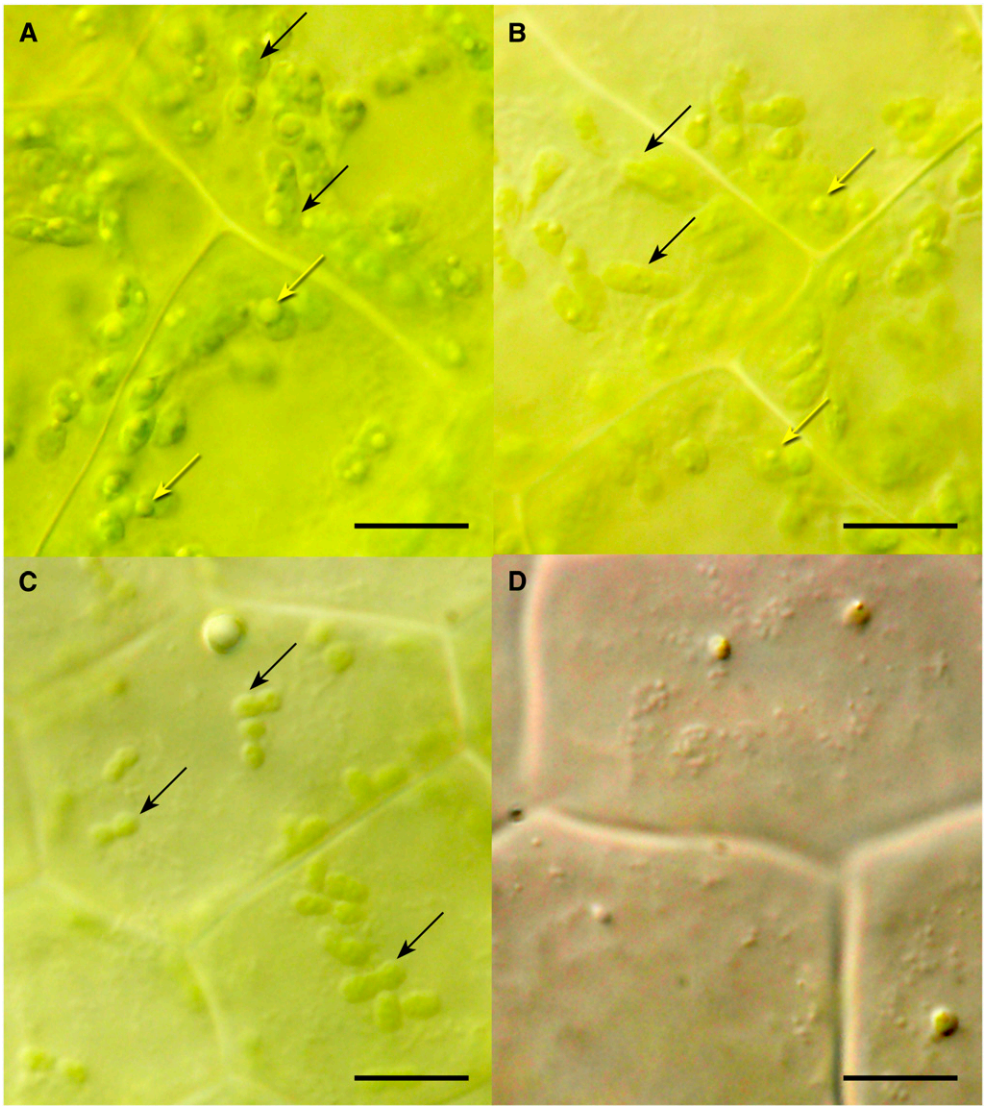

Fig. 2. Light micrographs of chloroplast changes in four stages of programmed cell death (PCD) within a single lace plant leaf. (A) Stage 1a. (B) Stage 2a. (C) Stage 3a. (D) Stage 4a. Bars = 10 μm. The chloroplasts and starch grains (yellow arrows) decreased in size and number with increasing PCD stage; dividing (dumbbell-shaped) chloroplasts (black arrows) were not observed during the last stage of PCD (4a) prior to PM collapse.

veins on either side of the midrib vein, which, along with a series of transverse veins, forms a lattice work of windows (Fig. 1B) and eventually perforations. The area between the outer two longitudinal veins on this leaf are often not yet true windows (i.e., longitudinal veins are close together and transverse veins are not apparent), and they may or may not eventually undergo PCD.

Four stages of PCD (1a–4a) within a leaf—The development of PCD in the lace plant leaf is most advanced closest to the midrib and the least advanced at the leaf edge. Thus, the window formation stage of lace plant growth could be subdivided into four PCD stages: (1) Stage 1a, cells on the meristematic leaf border, between the last two longitudinal veins, not undergoing PCD (referred to as non-PCD cells); (2) Stage 2a, first true window, interior to the second outermost longitudinal vein and the second least advanced stage of PCD; (3) Stage 3a, window interior to the third outermost longitudinal vein and the second most advanced stage of PCD; and (4) Stage 4a, the window closest to the midrib vein and the most advanced stage of PCD (i.e., the last stage prior to tonoplast rupture and PM collapse) (Fig. 1C).

Because some variability is found in the maturity within a row of windows (measured from leaf tip to petiole), it was ensured that the four windows selected, starting with the outer window leaf edge (Stage 1a) to the innermost window next to the midrib vein (Stage 4a), possessed a continual progression of PCD stages. Light microscope observations and measurements on a cellular level were performed using differential interference contrast (DIC) optics and a Nikon eclipse 90i compound microscope (Nikon Canada, Mississauga, Ontario, Canada) fitted with a digital camera (Nikon DXM 1200c) and using NIS-Elements imaging and analysis software. All observations and measurements with light microscopy (LM) were performed in vivo on epidermal cells of live samples. For the measurement of moving organelles and structures, 60-s time-lapse videos using 2-s intervals were used. Observations within each window were always made on the most advanced cells, located at the window center.

For six experimental replications (individual leaves, most from different plants), measurements were obtained at each stage of PCD. At a magnification of 480× (focal plane just below the PM), the cross-sectional area of 10 randomly selected cells was measured. At a magnification of 1200× (just below the PM), the average apparent cross-sectional area and maximum/minimum (max/min) feret diameter ratio [i.e., a variable that approximates how spherical or oblong an object is; a perfectly circular object equals 1, while an oblong object would be >1 [for a more detailed description, see Pyke and Page, 1998]) were measured for 10 chloroplasts selected randomly, and the number of chloroplasts within a 1000 μm^2 grid was counted. The cross-sectional area and number of all visible starch granules located on the 10 randomly selected chloroplasts were also measured. The rate of organelle movement can be inferred by measuring

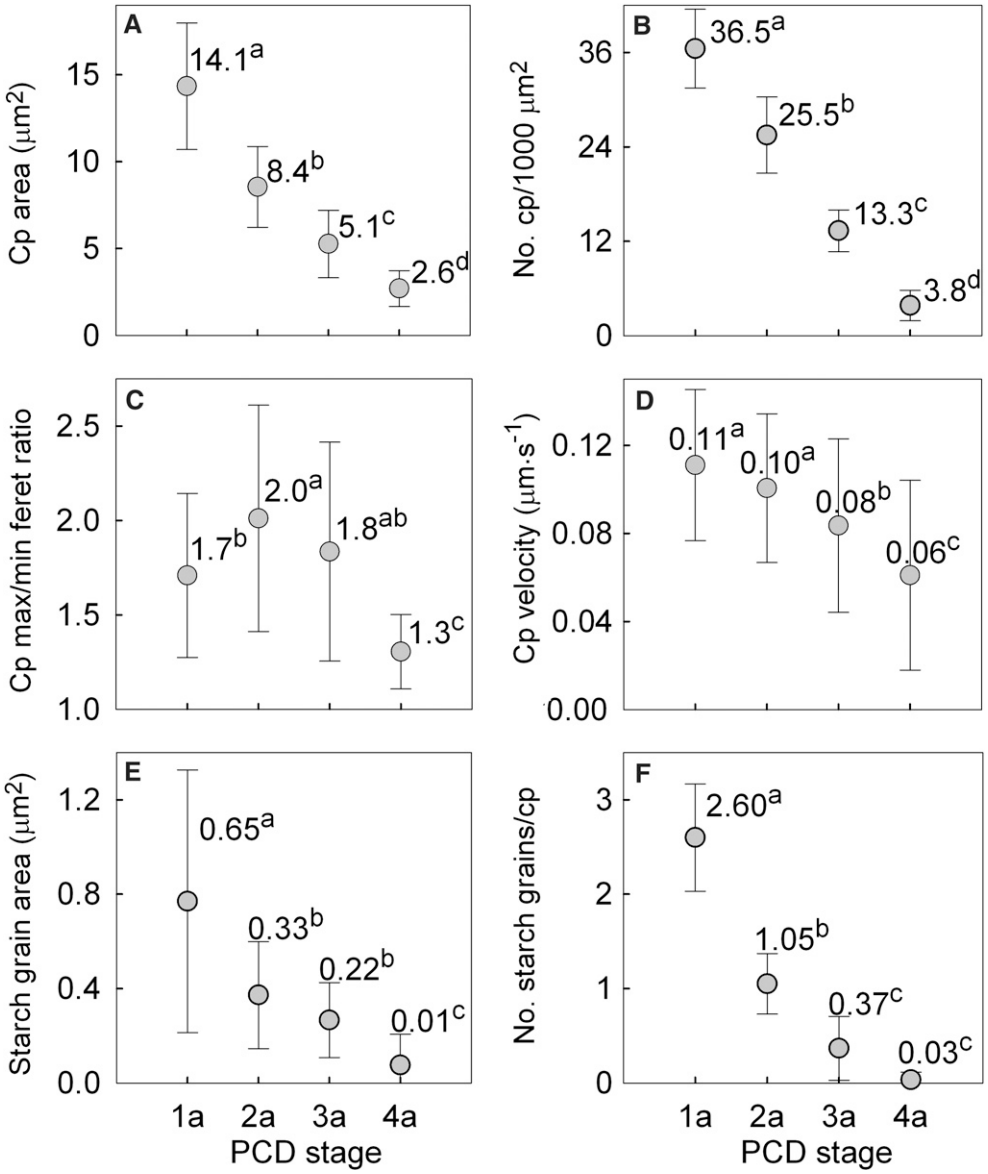

Fig. 3. Means and standard deviations at four programmed cell death (PCD) stages (1a–4a) within a lace plant leaf for (A) chloroplast (cp) area, (B) number of chloroplasts per 1000 μm², (C) chloroplast maximum/minimum feret diameter ratio, (D) chloroplast velocity, (E) starch grain area and (F) number of starch grains per chloroplast. Means with dissimilar letters are significantly different.

the time organelles take to cover a calibrated distance. The average velocity for chloroplasts and for mitochondria was calculated by measuring the distance (using a multipoint system) that 10 of the organelles moved, using 60-s time-lapse video clips. At a magnification of 1200× (focal plane further below the PM), the number of transvacuolar cytoplasmic strands, which often radiated from the nuclear region through the vacuole to the peripheral cytosol, observed during a 60-s time-lapse video, were counted in the entire field of view (FOV; 8000 μm²). At a magnification of 1200× (focal plane deep within the cell), the apparent cross-sectional area of any visible, circular nuclei, and the number of objects undergoing Brownian motion (i.e., random and erratic movement) within the vacuoles were evaluated using a 60-s time-lapse video. In addition, the apparent cross-sectional area of nuclei from cells with a collapsed PM (N = 20) was measured, and a sample (N = 20) of chloroplast areas was measured from the epidermal cells of two leaves at the mature perforation stage.

A balanced single-factor analysis of variance (ANOVA) (Minitab, Release 15, State College, Pennsylvania, USA) model was used to evaluate significant differences between means for the PCD stages for the following: cell area, chloroplast area, chloroplast max/min feret diameter, chloroplast number, chloroplast and mitochondria velocity, starch granule number, transvacuolar strand number, and object number in the vacuole. An unbalanced general linear model (GLM) (Minitab, Release 15) was used to determine if there was a significant difference between means at the various PCD stages for the number of starch granules and cross-sectional area of the nucleus. A t test (Minitab, Release 15) was used to compare the cross-sectional area of nuclei in cells at Stage 4a with the area from those in cells with a collapsed PM, the overall velocity of mitochondrial and chloroplast streaming, and chloroplast area in window formation compared to mature perforation leaves.

Three stages of PCD (1b–3b) within a window—A single window at mid to late formation could be subdivided into three PCD stages: (1) Stage 1b, non-PCD cells located within two cell layers of the encompassing veins; (2) Stage 2b, cells located midway between the surrounding veins and the window center undergoing PCD; and (3) Stage 3b, cells located in the window center that are in a late stage of PCD, but before tonoplast rupture and PM collapse (Fig. 1D). Experimental replications, measurements, and analysis for these three PCD stages were the same as just described for the stages within a leaf.

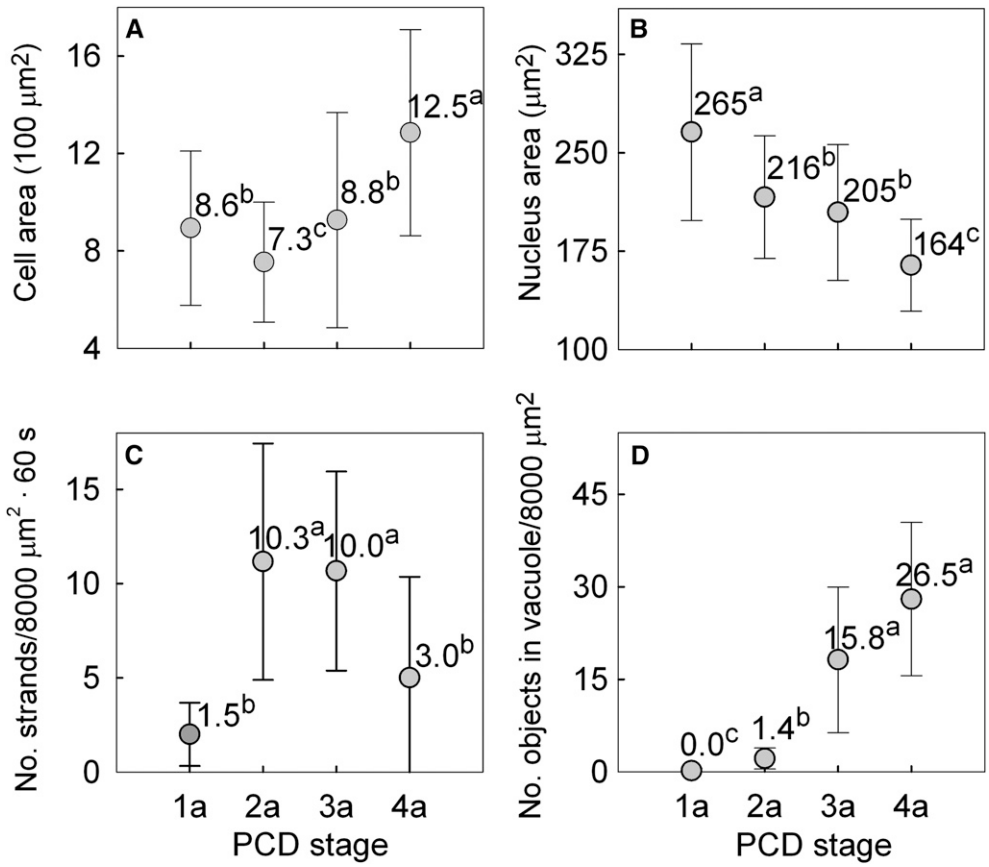

Fig. 4. Means and standard deviations at four programmed cell death (PCD) stages (1a–4a) within a lace plant leaf for (A) cell area, (B) nucleus cross-sectional area, (C) number of transvacuolar strands per 8000 μm²·60 s, and (D) number of objects in vacuole per 8000 μm². Means with dissimilar letters differ significantly.

PCD over time—Three detached lace plant leaves that continued to grow while floating in distilled water were monitored over two days. Measurements similar to those just described were performed on four non-PCD cells (cells within two cell layers of a vein) and four central cells undergoing PCD in each leaf. Window dimensions and area were also monitored on four windows in each replication. Regression analysis was used to determine significance in trends observed over time (Minitab, Release 15). A proc GLM homogeneity-of-slopes model (SAS, Release 8.0; SAS Institute, Cary, North Carolina, USA) was used to compare data sets.

Transmission electron microscopy (TEM)—Transmission electron micrographs were used to corroborate LM observations. Tissue samples (2 mm²) obtained from cells at the center (undergoing PCD) and periphery (i.e., non-PCD) of windows were prepared as described in Gunawardena et al. (2004). A Philips Tecnai 12 transmission electron microscope (Philips Electron Optics, Eindhoven, Netherlands) operated at 80 kV and fitted with a Kodak (Rochester, New York, USA) Megaview II camera with software (AnalySIS, Soft Imaging System, Münster, Germany) was used to generate images.

Statistics—Before statistical analysis, a normal probability plot (NPP) of the residuals and an Andersen–Darling test were used to test for normality; a fitted values vs. residuals plot was created to check for constant variance (Minitab, Release 15). When needed, correction factors were used. Means of individual treatments were compared using a least-squares means (LSmeans) comparison (SAS, Release 8.0). When a correction factor was used, the means were back-transformed. Significance was defined as $P < 0.05$.

Supplemental data—Videos and additional figures are available in Appendices S1–S13 in the Supplemental Data with the online version of this article.

RESULTS

Four stages of PCD (1a–4a) within a leaf—The average number and cross-sectional area of chloroplasts declined steadily with advanced stages of PCD (Figs. 2A–2D, 3A, 3B) ($F_{3,20} = 81.9$, $P < 0.001$; $F_{3,236} = 313.8$, $P < 0.001$); only a few, small, round chloroplasts were observed in the most advanced PCD stage (4a) (i.e., just before tonoplast rupture and PM collapse) (Fig. 2D). The number and size of light-colored spots, identified as starch granules, visible from the chloroplast surface also declined (Figs. 2A–2D, 3E, 3F) ($F_{3,20} = 56.9$, $P < 0.001$; $F_{3,245} = 40.6$, $P < 0.001$). Many chloroplasts had a dumbbell shape, typical of organelles dividing via elongation and constriction, even during the mid PCD stages (K. Osteryoung, Michigan State University, personal communication) (Fig. 2C; Appendix S1, see Supplemental Data with online version of this article). From observations and quantitative analysis combined, dividing chloroplasts typically had a max/min feret diameter ratio >1.8. The chloroplast max/min feret ratio first increased slightly and then decreased during the advanced stages of PCD (Fig. 3C) ($F_{3,236} = 23.5$, $P < 0.001$), indicating that some chloroplasts continued to form, or maintained, their elongated, dumbbell shape even as PCD progressed. However, very few dumbbell-shaped chloroplasts were observed during the most advanced stage of PCD (Fig. 2D). For comparison, the chloroplasts observed in mature perforation stage leaves were much larger (40.0 ± 6.8 μm²; $t = 18.0$, df = 22,

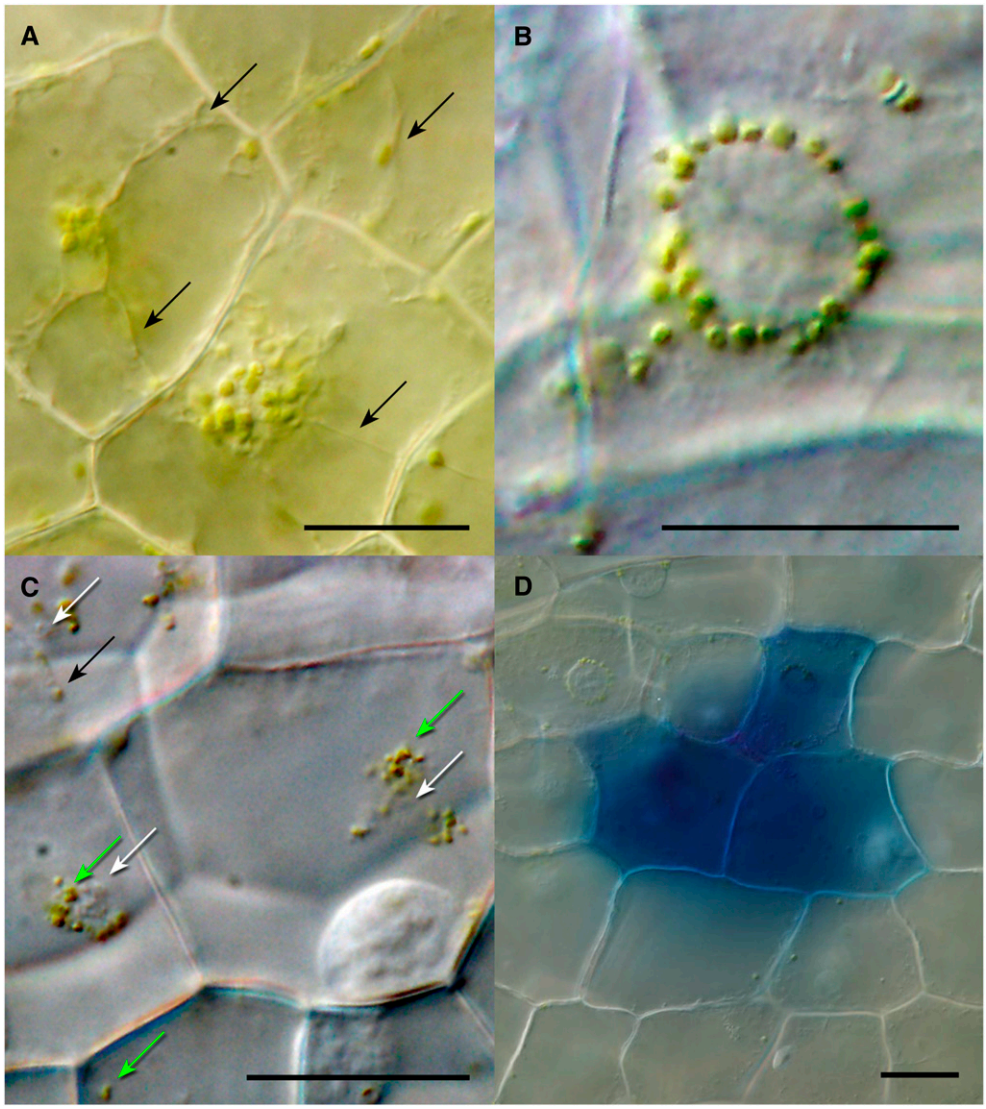

Fig. 5. Light micrographs of cellular features of lace plant programmed cell death (PCD) involved in development of leaf perforations. (A) Transvacuolar strands (arrows) (Stage 3a) (online Appendix S6). (B) Chloroplast ring formation (Stage 4a). (C) Conglomerates of objects, potentially intact chloroplasts or chlorophyll-containing plastoglobuli, in the vacuole undergoing Brownian motion (Stage 4a) (aquarium-grown). Green objects (green arrows) were more often located on the periphery of conglomerates; white objects (white arrows) were generally located in the center. Some shriveled chloroplasts remain next to nucleus (black arrow) (online Appendix S7). (D) Cells (Stage 4a) stained with Evans blue. Live cells remained clear; cells with ruptured tonoplast or collapsed plasma membrane stained blue. Bars = 20 μm.

$P < 0.001$), contained only small starch granules (data not shown), were rarely observed dividing (max/min feret diameter ratio = 1.15 ± 0.04), and were saucer-shaped (online Appendix S2).

The chloroplast streaming velocity (≈ 0.09 μm·s^{-1}) declined with increased PCD stage (Fig. 3D) ($F_{3,236}$ = 19.9, $P < 0.001$). Streaming of the mitochondria had a higher velocity (≈0.14 μm·s^{-1}) than that observed for the chloroplasts (t = 12.6, df = 472, $P < 0.001$) and appeared to be sustained, with no dramatic changes observed in the population or size (data not shown), even at very advanced stages of PCD (online Appendix S3). Mitochondrial streaming ceased just prior to (i.e., within minutes of) PM collapse (online Appendix S4), likely as a result of tonoplast rupture. Cells during the stage of PCD after cessation of streaming, but before PM collapse, were stained light blue with Evans blue (data not shown).

With the exception of the non-PCD leaf cells (Stage 1a), the mean cross-sectional area of the cells increased with increasing PCD stage ($F_{3,236}$ = 23.0, $P < 0.001$) (Fig. 4A). The cross-sectional area of the nuclei decreased with increasing stage of PCD ($F_{3,75}$ = 14.1, $P < 0.001$) (Fig. 4B). In cells that had already undergone PM collapse (not included in the four PCD stages), the mean nucleus cross-sectional area (99.7 ± 27.0 μm^2) was significantly smaller than the nucleus area in the most advanced stage observed (Stage 4a) before PM collapse (t = 6.7, df = 40, $P < 0.001$). In a side study where plasmolysis in cells in the advanced stages of PCD was hastened via dehydration, the tonoplast seemed to rupture first, based on the rapid shrinkage of the nucleus and simultaneous cessation of mitochondrial streaming, and was quickly followed (i.e., in a few minutes) by PM collapse (online Appendix S5).

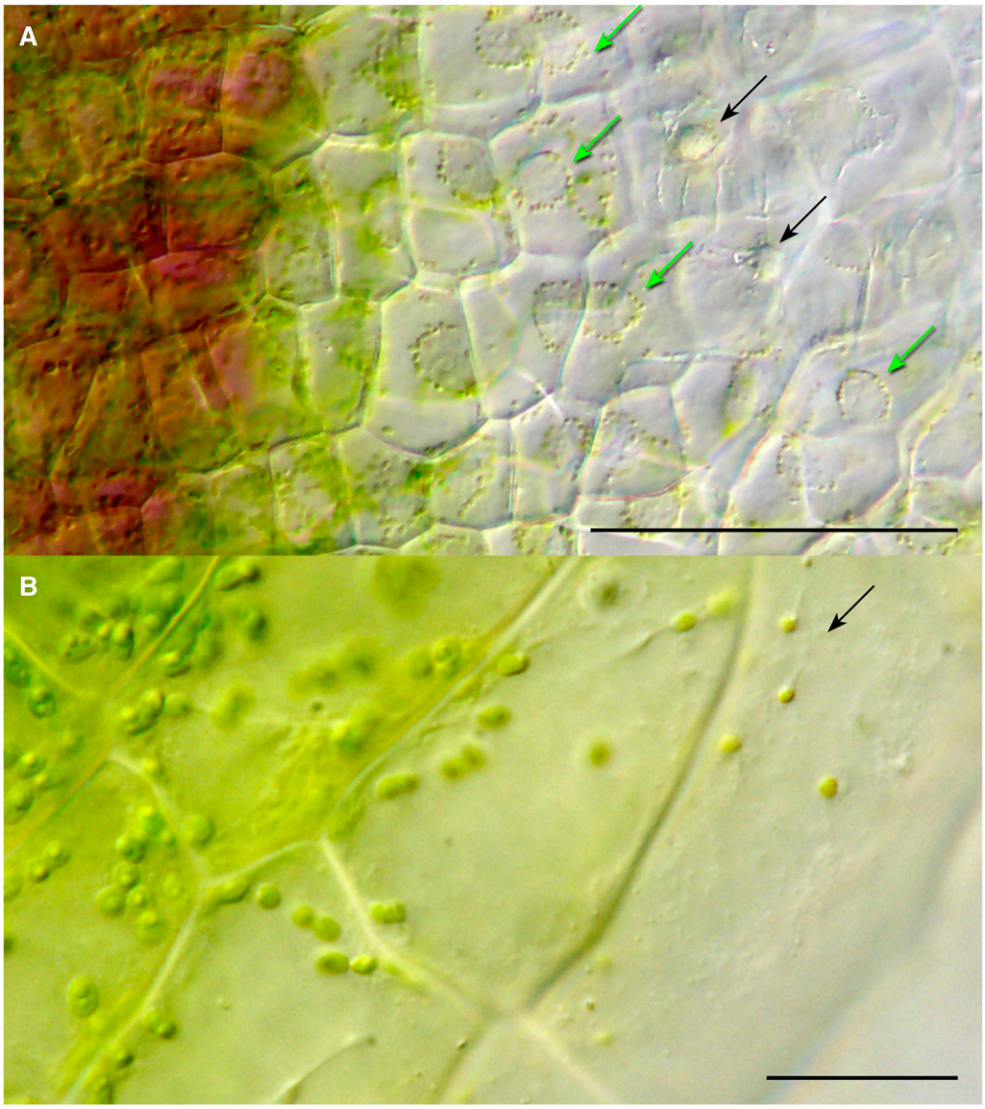

Fig. 6. Light micrographs showing a gradient of programmed cell death (PCD) stages within a single lace plant window. (A) Black arrows point to condensed nuclei in cells with ruptured tonoplast and plasma membrane; green arrows point to rings of chloroplasts. (B) Arrow points between two recently divided chloroplasts, each trailing a strand of viscous material at an advanced stage of PCD (see video in online Appendix S8). In (A) and (B), the vein and non-PCD cells are located to the left, and center cells are to the right. Bars = (A): 100 μm, (B): 20 μm.

The number of transvacuolar strands, which often appeared to be associated with chloroplasts and chloroplast movement (Fig. 5A; online Appendix S6), was greatest during the mid PCD stages. The number of strands declined during the late PCD stages ($F_{3,20} = 5.2$, $P = 0.008$) (Fig. 4C). As the number of strands declined (Stage 3a–4a), the remaining chloroplasts congregated, or were more easily observed due to a reduction in anthocyanin content, in a ring formation around the nucleus (Figs. 5B, 6A).

The number of objects undergoing Brownian motion inside the vacuole increased dramatically with increased PCD stage ($F_{3,20} = 36.3$, $P < 0.001$) (Fig. 4D). Observed singly and in low numbers during the early stages of PCD, the objects formed conglomerates of plastid-like structures during the later PCD stages. Objects were often white, though some were green, likely indicating the presence of chlorophyll (Fig. 5C; online Appendix S7). Interestingly, green objects were more often observed in aquarium-grown plants than in those grown in magenta boxes (data not shown); objects toward the center of conglomerates were often white, while those on the periphery were more often green (Fig. 5C; online Appendix S7).

Three stages of PCD (1b–3b) within a window—Individual windows contained a gradient of PCD stages (Fig. 6; online Appendix S8). Cells close to the vein contained red anthocyanin, but the red color was rather abruptly absent in cells toward the center of the window (Figs. 1D, 6A). Cells close to the vein generally had numerous large chloroplasts, while cells closer to the window center, including cells just before and after PM collapse, contained few to none (Fig. 6). All the parameters measured, except for mitochondria streaming velocity, differed significantly between the PCD stages (data not shown, $P < 0.001$). The trends found between PCD Stages 1b–3b reflected those in Stages 1a–4a of the previous experiment (online Appendices S9, S10).

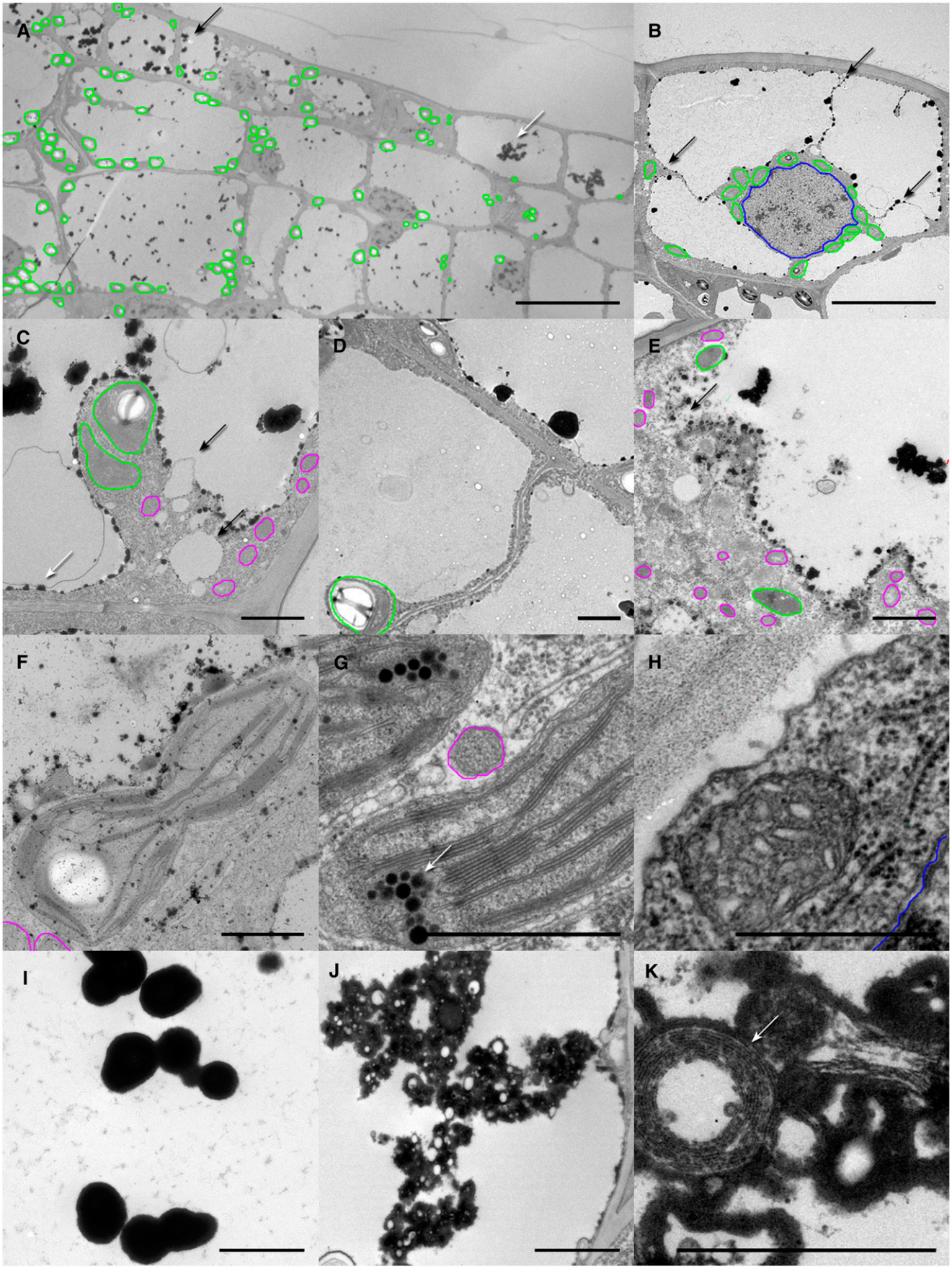
A
B
C
D
E
F
G
H
I
J
K

PCD over time—Leaf elongation averaged ≈2.7 ± 0.5 mm·day^{-1} (N = 3) over two days in the detached leaves. Cell division continued in non-PCD cells, but not center cells (data not shown), while PCD progressed in the latter (online Appendix S11). Because the leaves were periodically exposed to air, some microbes were present. Microbes appeared to be preferentially attracted to window center cells in advanced stages of PCD, likely as a result of leakage. Trends observed over time were similar to those observed over the four stages within a leaf and the three stages within a window (data not shown). Two notable exceptions were that the starch granule area had a diurnal pattern in the non-PCD cells and a low, but increasing, number of objects were undergoing Brownian motion in the non-PCD cell vacuoles (online Appendix S12). The center cell area increased by approximately twice that of the overall window, while the window increased in area by approximately twice that of the peripheral non-PCD cells (online Appendix S13).

TEM—Several of the LM observations were corroborated with TEM. Chloroplast density was greater in the peripheral non-PCD cells than in the center cells (Fig. 7A). Transvacuolar strands were commonly observed in cells in the middle stages of PCD and often emanated from the nucleus to just below the PM (Fig. 7B). Figure 7B also shows the ring of chloroplasts around the nucleus commonly observed with LM during the mid to late stages of PCD (Fig. 5B). The chloroplasts caused slight indentations in the nucleus (Fig. 7B). What appeared to be viable chloroplasts were often observed entering the vacuole (Fig. 7C); however, because TEM samples are static, it is impossible to tell whether these images had captured the initial stage of autophagic chloroplast destruction or whether the chloroplasts were simply traveling through transvacuolar strands that passed through the vacuole (Figs. 7C and 7D).

Cells in an advanced stage of PCD were sometimes observed with a ruptured tonoplast while the PM remained intact (Fig. 7E); however, such observations were infrequent, possibly indicating the small window of time over which cells remained in this state. Dumbbell-shaped chloroplasts, similar to those observed with LM (Fig. 2A–2C), were confirmed to be chloroplasts dividing via constriction (Fig. 7F), not simply two chloroplasts next to one another. Dividing chloroplasts were observed in non-PCD cells as well as in cells in the early to mid stages of PCD.

Chloroplasts often contained large starch granules (most prominent in non-PCD cells, but also observed in mid stage PCD cells (Fig. 7F)), highly defined thylakoid structures (Fig. 7F, 7G), and oil bodies called plastoglobuli (Fig. 7G). Although mitochondria were often observed with identifiable cristae, even at an advanced stage of PCD (Fig. 7H), the thylakoid structure observed in chloroplasts became less distinct (data not shown).

Several seemingly discrete categories of objects were observed inside the cell vacuoles. Globular bodies, presumably oil or something equally electron-dense, were frequently observed in non-PCD cell vacuoles, particularly in the epidermal cells, but were found far less often in the center cells undergoing PCD (Fig. 7A). These globular bodies were generally observed singly, though in high concentrations, and did not form conglomerate structures (Fig. 7I). It is important to note that these objects were never observed with LM, which also opens the possibility that they are artifacts of fixation. Conglomerates of what appeared to be membrane-bound or plastid-like objects (Fig. 7J, 7K) were frequently observed in the vacuoles of center cells undergoing PCD, but not in non-PCD cells (Fig. 7A). This second category of objects appeared, in structure and size, to be the same as those observed during the mid to late PCD stages with LM (Fig. 5C; online Appendix S7). A third category of objects was ubiquitous just inside the tonoplast membrane (Fig. 7C, 7E).

DISCUSSION

In this in vivo analysis of the lace plant during developmental PCD, we found that the process in this plant shares several interesting features with other more widely studied models of cell death, but also has some clear distinctions.

Lace plant developmental PCD execution sequence—While cells in the periphery of the window primarily expand and continue to divide in the direction parallel to the nearest vein, center cells lose volume while they are stretched in all directions (online Appendix S13). The decrease in nucleus cross-sectional area prior to tonoplast collapse (Fig. 4B) might indicate a decrease in nucleus volume, but may also reflect a change in shape, as in the *Zinnia* model (Obara et al., 2001). The decrease in nucleus cross-sectional area after tonoplast collapse might result from chromatin condensation. In the *Zinnia* model the rupture of the tonoplast results in immediate cessation of cytoplasmic streaming (Groover et al., 1997; Jones et al., 2001) and triggers the rapid degradation of the nucleus, which takes 10–20 min (Obara et al., 2001). Evidence for mega-autophagy, before PM collapse, was also found in the lace plant (Figs. 5D, 7E; online Appendices S4, S5). The PCD processes in the lace plant, based on the current study's findings, are summarized in Fig. 8.

←

Fig. 7. Transmission electron micrographs of fixed leaf tissue of lace plant at different stages of programmed cell death (PCD) involved in the development of leaf perforations. (A) Concave nature of lace plant leaf at a mid PCD stage; chloroplasts (outlined in green) and starch grains over varying stages of PCD: non-PCD cells (left, least advanced PCD) and center cells (right, most advanced PCD). Conglomerates of objects (potentially condensed chloroplasts or gerontoplasts) (white arrow) were observed in the vacuoles of center cells undergoing PCD; unidentified globular bodies (black arrow) were also observed inside the vacuoles of many cells, most frequently in non-PCD cells. (B) Mid stage center cell—transvacuolar strands (arrows) and chloroplast (outlined in green) ring formation around nucleus (outlined in blue). (C) Mid stage center cell—chloroplasts (outlined in green), one with obvious starch grain, entering vacuole with vesicles (black arrows), mitochondria (outlined in magenta) and electron-dense material just interior to the tonoplast (white arrow). (D) Mid stage center cell—solitary chloroplast (outlined in green) with starch grain at the end of a long transvacuolar strand. (E) Late stage center cell—tonoplast rupture (arrow) and intact PM with mitochondria (outlined in magenta) and chloroplast (outlined in green). (F) Mid stage center cell—a dividing chloroplast with starch grain and visible thylakoid membranes next to two mitochondria (outlined in magenta). (G) Non-PCD cell—two chloroplasts showing oil bodies (or plastoglobuli) (arrow) and thylakoid structure next to a mitochondrion (outlined in magenta). (H) Late stage center cell—a mitochondrion and ER next to nucleus (outlined in blue). (I) Non-PCD cell—unidentified globular objects in vacuole. (J) Late stage center cell—a conglomerate of objects inside vacuole identified as chloroplast material. (K) Late stage center cell—objects in vacuole showing apparent distorted thylakoid or membranous structures (arrow). Bars = (A): 30 μm, (B): 10 μm, (C, D, E, I, J): 2 μm, (F, G, H, K): 1 μm.

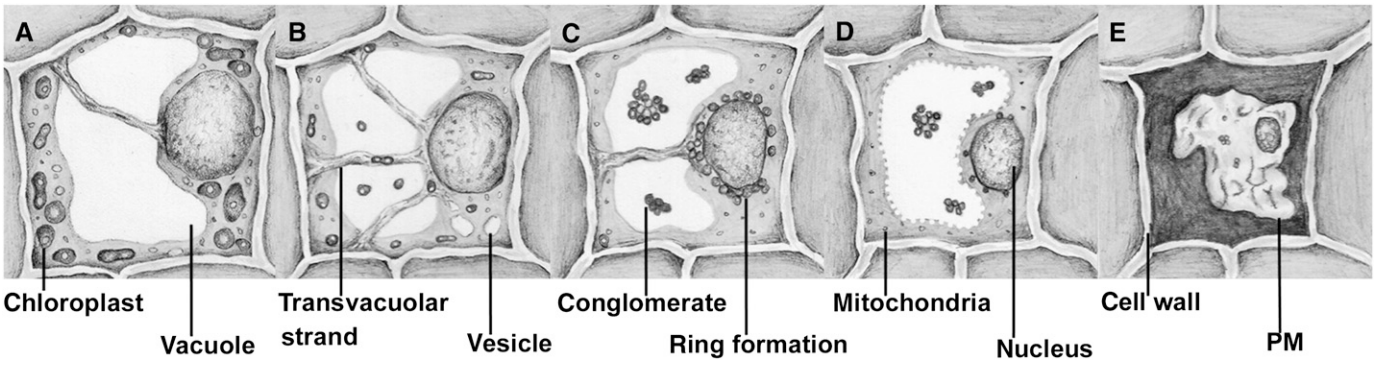

Fig. 8. Illustration of events during programmed cell death (PCD) involved in the development of perforations in leaf of lace plant. (A) Healthy cell: chloroplasts are large and numerous with large starch grains; some chloroplasts are undergoing division (shown as dumbbell-shaped chloroplasts); mitochondria are numerous and maintain their size throughout PCD; there is a large central vacuole and nucleus. (B) Chloroplast and starch grain number and size decrease as they do for the remainder of PCD; chloroplast division continues and possibly increases; a few individual objects, potentially intact chloroplasts or plastoglobuli, some of which contain chlorophyll, undergo Brownian motion inside the vacuole; there is an increase in the appearance of transvacuolar strands (often associated with the travel of chloroplasts); some vesicle formation is evident. (C) There is a decrease in the appearance of transvacuolar strands; remaining small, spherical chloroplasts form a ring around the nucleus; conglomerates of objects undergo Brownian motion inside the vacuole. (D) A sudden cessation of mitochondrial streaming, followed by a rapid shrinkage of the nucleus over the course of 15–20 min, is thought to be caused by tonoplast rupture; Brownian motion of objects in conglomerates continues; there is no evidence of transvacuolar strands. (E) Plasma membrane collapses and the perforation formation stage begins. The overall process is estimated to take ~2 d, depending on conditions. Events from D through E are rapid and are estimated to take ~15–20 min.

Chloroplast fate—The decrease in lace plant chloroplast size, number, and structure before the collapse of the cell is different from the sequence observed during PCD in the *Zinnia* leaf mesophyll TE system, where chloroplasts remain intact until tonoplast rupture and the apparent release of hydrolases (Kuriyama, 1999; Fukuda et al., 1998). However, the fate of chloroplasts during lace plant PCD is reminiscent of senescing leaf cells. In senescing leaves, the internal grana and thylakoid structure often disappears (Ljubesic, 1968; Inada et al., 1998, 1999; Sakamoto, 2006; Hörtensteiner and Lee, 2007), and chloroplast number (Ono et al., 1995; Matile, 2001), chloroplast size (Inada et al., 1998, 1999) and starch granule size (Matile, 2001) decreases before the onset of cell death.

Chloroplasts typically assume a dumbbell shape when actively dividing (Pyke and Page, 1998; Osteryoung and Nunnari, 2003). Such actively dividing chloroplasts were frequent at Stages 1a and 2a of PCD, but became progressively rarer at later stages. It is unknown whether chloroplasts continued to initiate division during the middle stages of PCD. At the very least, it is believed that once division was initiated, chloroplasts continued to divide during PCD.

Evidence for autophagy?—It is presently not known what the relationship might be, if any, between the three categories of objects observed inside the vacuoles: (1) globular bodies observed singly in non-PCD cells (Fig. 7I), (2) conglomerates containing chlorophyll and membrane material in the center cells undergoing PCD (Figs. 5C, 7J, 7K), and (3) electron-dense material often observed just inside the tonoplast membrane (Fig. 7C). Many cells contained what appeared to be vesicles, both inside and outside the vacuole (Fig. 7C), as well as the remnants of membranes or possibly even intact organelles inside the vacuole (Figs. 5C, 7A, 7J, 7K; online Appendix S7) during late stage PCD. This evidence suggests active micro- and macro-autophagy, respectively (Phillips et al., 2008). Microautophagy occurs during normal turnover of cell constituents, but during senescence the presence of materials in the vacuoles might suggest that autophagy is upregulated to such a degree that the rate of transport of materials to the vacuole is higher than the rate of degradation inside the vacuole (Matile, 1992, 1997).

The presence of green material in the vacuole, presumed to be chlorophyll (Fig. 5C; online Appendix S7), can be explained, it seems, in only two ways. One is the transfer of entire chloroplasts, at some stage where they still contain chlorophyll, to the vacuole. Only a few previous reports are suggestive of such a phenomenon (Wittenbach et al., 1982; Minamikawa et al., 2001), and the suggestion is considered controversial (Matile, 1992, 1997). The other explanation is that plastoglobuli, known to contain chlorophyll and degradation products from membranes (Hörtensteiner and Feller, 2002), move from the chloroplasts to the vacuole. Plastoglobuli have been observed to leave the chloroplasts (Guiamet et al., 1999), but their fate is unknown.

Are chloroplasts involved in triggering PCD?—During the later stages of lace plant PCD, most remaining chloroplasts were observed around the nucleus (Figs. 5B, 6A) and formed indents in the nuclear periphery (Fig. 7B). In a study on tobacco cells subjected to osmotic stress, chloroplasts were also observed in increased numbers around the nucleus and were found in what was termed a "nuclear pouch" (Reisen et al., 2005). It may be that in tobacco and lace plant, the chloroplasts simply accumulated, or were spared, in this nuclear pouch. However, it would be tempting to hypothesize that the closeness of the two organelles is due to competition of chloroplasts for a substance from the nucleus, which delays their internal degradation or that the chloroplasts somehow play an integral role in the PCD process.

Some evidence suggests that chloroplasts may be responsible for PCD regulation. In tobacco plants with the plastid *ndhF* gene knocked out, the time until leaf cell PCD (visible senescence) was drastically delayed (Zapata et al., 2005), indicating that chloroplasts can induce normal PCD. Other data indicate

that chloroplasts promote PCD induced by cyanide (Samuilov et al., 2003) and that chloroplasts may play a role in heat-induced PCD (Doyle and McCabe, 2007). In plants, chloroplasts are among the main generators of reactive oxygen species (ROS) (Zapata et al., 2005; Asada, 2006). Elevated ROS levels have been shown to induce PCD (Jabs, 1999; Kombrink and Schmelzer, 2001) and have been linked to chloroplast degradation in senescing leaves (Rosenvasser et al., 2006) and to lace plant cells undergoing PCD (Gunawardena et al., 2007). The present data implicate the role of chloroplasts in PCD; however, the exact role is unclear.

Conclusions—Despite its importance, PCD in plants has been studied in detail in only a few types of tissues and cells. The morphology of its leaf (thin cuticle and only four cell layers thickness) and the predictability of cell death (both in timing and location) makes the lace plant an excellent model for microscopic investigations on in vivo changes during developmental PCD.

The data suggest PCD in lace plants may be associated with an upregulation of autophagic activity, although we have not shown the explicit presence of autophagosomes in the cytoplasm. An increase in macro-autophagy was mainly indicated by the presence of numerous vesicles and membranes inside the vacuoles. Mega-autophagy, the cause of cell death, was shown by rupture of the tonoplast and the subsequent rapid disappearance of what remained of the cells. Chloroplast numbers significantly declined in number and size prior to tonoplast collapse. In the present system, the majority of chloroplasts thus do not become dismantled via mega-autophagy. Although controversial, circumstantial evidence of chlorophyll-containing membranous material inside the vacuole suggests intact chloroplasts may be enveloped by the vacuole, but the present data are not conclusive enough to state this definitively.

The observation that chloroplasts accumulated around the nucleus at a rather late stage of PCD appears to be novel. The discernment of the lace plant's PCD execution process, in particular the role of the chloroplast, in the present study is the most detailed to date. Leaf senescence and the *Zinnia* TE and lace plant models all share many of the hallmarks of PCD. However, the fate of the chloroplasts in lace plant before tonoplast collapse is reminiscent of leaf senescence but distinct from PCD in the *Zinnia* model, while the well-defined and localized nature of the cell death in lace plant is more similar to that observed in differentiating TEs and distinct from large scale, organ-based senescence.

LITERATURE CITED

ASADA, K. 2006. Production and scavenging of reactive oxygen species in chloroplasts and their functions. *Plant Physiology* 141: 391–396.

BALK, J., AND C. J. LEAVER. 2001. The PET1-CMS mitochondrial mutation sunflower is associated with premature programmed cell death and cytochrome *c* release. *Plant Cell* 13: 1803–1818.

DOYLE, S., AND P. MCCABE. 2007. Can chloroplasts regulate programmed cell death? *Comparative Biochemistry and Physiology* 146: C.2.13.

FUKUDA, H., Y. WATANABE, H. KURIYAMA, S. AOYAGI, M. SUGIYAMA, R. YAMAMOTO, T. DEMURA, AND A. MINAMI. 1998. Programming of cell death during xylogenesis. *Journal of Plant Research* 111: 253–256.

GROOVER, A., N. DEWITT, A. HEIDEL, AND A. JONES. 1997. Programmed cell death of plant tracheary elements differentiating in vitro. *Protoplasma* 196: 197–211.

GUIAMET, J. J., E. PICHERSKY, AND L. D. NOODÉN. 1999. Mass exodus from senescing soybean chloroplasts. *Plant & Cell Physiology* 40: 986–992.

GUNAWARDENA, A. H. L. A. N. 2008. Programmed cell death and tissue remodelling in plants. *Journal of Experimental Botany* 59: 445–451.

GUNAWARDENA, A. H. L. A. N., J. S. GREENWOOD, AND N. G. DENGLER. 2004. Programmed cell death remodels lace plant leaf shape during development. *Plant Cell* 16: 60–73.

GUNAWARDENA, A. H. L. A. N., J. S. GREENWOOD, AND N. G. DENGLER. 2007. Cell wall degradation and modification during programmed cell death in lace plant, *Aponogeton madagascariensis* (Aponogetonaceae). *American Journal of Botany* 94: 1116–1128.

GUNAWARDENA, A. H. L. A. N., C. NAVACHANDRABALA, M. KANE, AND N. G. DENGLER. 2006. Lace plant: A novel system for studying developmental programmed cell death. *In* J. A. T. da Silva [ed.], Floriculture, ornamental and plant biotechnology advances and topical issues, 157–162. Global Science Books, Middlesex, UK.

HÖRTENSTEINER, S., AND U. FELLER. 2002. Nitrogen metabolism and remobilization during senescence. *Journal of Experimental Botany* 53: 927–937.

HÖRTENSTEINER, S., AND D. W. LEE. 2007. Chlorophyll catabolism and leaf coloration. *In* S. Gan [ed.], Senescence processes in plants, 108–144. Blackwell, Oxford, UK.

INADA, N., A. SAKAI, H. KUROIWA, AND T. KUROIWA. 1998. Three-dimensional analysis of the senescence program in rice (*Oryza sativa* L.) coleoptiles. Investigations of tissues and cells by fluorescence microscopy. *Planta* 205: 153–164.

INADA, N., A. SAKAI, H. KUROIWA, AND T. KUROIWA. 1999. Senescence program in rice (*Oryza sativa* L.) leaves: Analysis of the blade of the second leaf at the tissue and cellular levels. *Protoplasma* 207: 222–232.

JABS, T. 1999. Reactive oxygen species as mediators of programmed cell death in plants and animals. *Biochemical Pharmacology* 57: 231–245.

JONES, A. M., A. GROOVER, X. YU, AND T. PERDUE. 2001. Final and fatal step of tracheary element differentiation. *In* N. Morohoshi and A. Komamine [eds.], Molecular breeding of woody plants, 29–42. Elsevier, Amsterdam, Netherlands.

KOMBRINK, E., AND E. SCHMELZER. 2001. The hypersensitive response and its role in local and systemic disease resistance. *European Journal of Plant Pathology* 107: 69–78.

KURIYAMA, H. 1999. Loss of tonoplast integrity programmed in tracheary element differentiation. *Plant Physiology* 121: 763–774.

LJUBESIC, N. 1968. Feinbau der Chloroplasten während der Vergilbung und der Wiederergrünung der Blätter. *Protoplasma* 66: 369–379.

MATILE, P. 1992. Chloroplast senescence. *In* N. R. Baker, and H. Thomas [eds.], Crop photosynthesis: Spatial and temporal determinants, 413-440. Elsevier, Amsterdam, Netherlands.

MATILE, P. 1997. The vacuole and cell senescence. *In* J. A. Callow [ed.], Advances in botanical research, vol. 25, 87–112. Academic Press, San Diego, California, USA.

MATILE, P. 2001. Senescence and cell death in plant development: Chloroplast senescence and its regulation. *In* E. M. Aro and B. Andersson [eds.], Regulation of photosynthesis, 277–296. Kluwer, Dordrecht, Netherlands.

MINAMIKAWA, T., K. TOYOOKA, T. OKAMOTO, I. HARA-NISHIMURA, AND M. NISHIMURA. 2001. Degradation of ribulose-bisphosphate carboxylase by vacuolar enzymes of senescing French bean leaves: Immunocytochemical and ultrastructural observations. *Protoplasma* 218: 144–153.

OBARA, K., H. KURIYAMA, AND H. FUKUDA. 2001. Direct evidence of active and rapid nuclear degradation triggered by vacuole rupture during programmed cell death in *Zinnia. Plant Physiology* 125: 615–626.

ONO, K., H. HASHIMOTO, AND S. KATOH. 1995. Changes in the number and size of chloroplasts during senescence of primary leaves of wheat grown under different conditions: Environmental and stress responses. *Plant and Cell Physiology* 36: 9–17.

OSTERYOUNG, K. W., AND J. NUNNARI. 2003. The division of endosymbiotic organelles. *Science* 302: 1698–1704.

PHILLIPS, A. R., A. SUTTANGKAKUL, AND R. D. VIERSTRA. 2008. The ATG12-conjugating enzyme ATG10 is essential for autophagic vesicle formation in *Arabidopsis thaliana. Genetics* 178: 1339–1353.

PYKE, K. A., AND A. M. PAGE. 1998. Plastid ontogeny during petal development in *Arabidopsis. Plant Physiology* 116: 797–803.

REISEN, D., F. MARTY, AND N. LEBORGNE-CASTEL. 2005. New insights into the tonoplast architecture of plant vacuoles and vacuolar dynamics during osmotic stress. *BMC Plant Biology* 5: 13.

ROSENVASSER, S., S. MAYAK, AND H. FRIEDMAN. 2006. Increase in reactive oxygen species (ROS) and in senescence-associated gene transcript (SAG) levels during dark-induced senescence of *Pelargonium* cuttings, and the effect of gibberellic acid. *Plant Science* 170: 873–879.

SAKAMOTO, W. 2006. Protein degradation machineries in plastids. *Annual Review of Plant Biology* 57: 599–621.

SAMUILOV, V. D., E. M. LAGUNOVA, S. A. GOSTIMSKY, K. N. TIMOFEEV, AND M. V. GUSEV. 2003. Role of chloroplast photosystems II and I in apoptosis of pea guard cells. *Biochemistry, Biokhimiia* 68: 912–917.

VAN DOORN, W. G., AND E. J. WOLTERING. 2004. Senescence and programmed cell death: Substance or semantics? *Journal of Experimental Botany* 55: 2147–2153.

VAN DOORN, W. G., AND E. J. WOLTERING. 2005. Many ways to exit? Cell death categories in plants. *Trends in Plant Science* 16: 117–122.

WITTENBACH, V. A., W. LIN, AND R. R. HEBERT. 1982. Vacuolar localisation of proteases and degradation of chloroplasts in mesophyll protoplasts from senescing primary wheat leaves. *Plant Physiology* 69: 98–102.

ZAPATA, J. M., A. GUÉRA, A. ESTEBAN-CARRASCO, M. MARTÍN, AND B. SABATER. 2005. Chloroplasts regulate leaf senescence: Delayed senescence in transgenic *ndhF*-defective tobacco. *Cell Death and Differentiation* 12: 1277–1284.